Effect of long-term hydrogen exposure on the mechanical properties of polymers used for pipes and tested in pressurized hydrogen

Sylvie Castagnet*, Jean-Claude Grandidier, Mathieu Comyn, Guillaume Benoît

Institut P' (UPR CNRS 3346), CNRS-ENSMA-Université de Poitiers, Département de Physique et Mécanique des Matériaux, ENSMA, 1 Avenue Clément Ader, BP40109, 86961 Futuroscope cedex, France

ABSTRACT

The influence of long-term exposure to hydrogen on the mechanical properties of polymers needs to be characterized for a reliable design of storage or transport facilities. However, mechanical tests in hydrogen atmosphere have been rarely reported. In the present study, two possible effects of hydrogen on tensile properties have been investigated in two polymers currently used for gas transport i.e. polyethylene (PE) and polyamide 11 (PA11): the mechanics-diffusion coupling and the influence of long-term exposure to hydrogen. Tensile tests in hydrogen atmosphere (30 bars) and atmospheric air at room temperature were compared, in the as-received materials as well as after aging in various conditions (pressure, temperature and duration). Results showed that the influence of hydrogen was prevalent neither on the tensile behavior nor on microstructure changes. This suggested that the design of hydrogen-dedicated parts could be based on data obtained in atmospheric air, even for long-term use.

© 2011 Elsevier Ltd. All rights reserved.

1. Introduction

Some polymers like polyethylene (PE) have been used for gas piping for a long time. In such applications, polymers are exposed to methane and methane-based mixtures. For a few years, hydrogen is being considered as a possible energetic vector, alternately to fossil energies. A great deal of effort is being expended in storage and networking issues for which materials properties characterization is crucial. In metals, hydrogen embrittlement processes are known to affect the strength and structural integrity [1–3]. Several models coupling hydrogen diffusion and mechanics have been proposed to analyze and predict hydrogen-induced cracking [4–6]. The design of parts like pipes requires quantitative data about the influence of pressurized hydrogen on the mechanical properties on one side, and about the influence of long-term exposure on the other side. However, such effects have not been investigated a lot in polymers so far.

In a general way, three main phenomena are bound to be addressed in polymers when used in a gas or liquid environment for very long durations. Firstly, in the same way as temperature, pressure or time, the diffusion of gas or liquid molecules into the polymer modifies the macromolecular mobility and subsequently the mechanical properties among which stiffness. Plasticization is the best known example, whatever on purpose, by incorporating a plasticizer into the polymer formulation, or as a spontaneous process, for instance by water sorption into hydrophilic polymers like polyamides [7–9]. Therefore, gas transport properties have been widely investigated in various gas/polymer systems, among which hydrogen [10] into PE or polyamide 11 (PA11) [11–14]. Secondly, physical aging is bound to occur during long-term use, mainly in glassy amorphous polymers but also in semi-crystalline ones due to the high degree of constraint sustained by the amorphous phase connected to the crystalline skeleton [15,16]. Effects of physical aging on the gas permeation properties were reported in various gases [17–19], showing a decrease of permeability but an increase of selectivity. Thirdly, degradation processes may arise from the exposure to chemically active gas or liquids. A dense literature, beyond the scope of this paper, has been published about the chemical and physical mechanisms associated with long-term exposure to nocive environment like UV [19] or gamma [20] radiation, but also to fuels [21], weak acids like carbon dioxide [22], chlorinated water [23] and oxygen [24,25]. Regarding the two polymers studied in the present paper, most studies addressed water hydrolysis [22] and oxidative induction times (OIT) [26], with a special interest paid on the kinetics and influence factors of antioxidants loss [25,26].

* Corresponding author. Tel.: +33 549 498 226; fax: +33 549 498 238.
E-mail addresses: sylvie.castagnet@ensma.fr, sylvie.castagnet@cnrs.pprime.fr (S. Castagnet).

Each of the above depicted phenomena is bound to influence directly the mechanical properties, as a consequence of molecular mobility and/or crystalline microstructure changes. This was often tracked from Dynamic Mechanical Analysis (DMA) experiments, however more in order to detect relaxation transitions [7,9–11] than to quantify mechanical moduli. Except for a few works based on flexural loading or impact [8,21], most studies were in uniaxial tension [19,20] and widely focused on static properties and ultimate properties (elongation at break, fracture mode) [8]. Most of the time, mechanical tests were performed ex-situ, after aging or exposure to gas atmosphere, and very rarely in liquid or gas directly [27–30]. In particular, and despite the current interest for hydrogen as a future energy, no data are available to evaluate the coupling between mechanical behavior and hydrogen diffusion into thermoplastics, and the influence on long-term exposure. However, due to the drastic safety standard associated with hydrogen transport, the design of hydrogen-exposed parts like pipes cannot be foreseen without any guarantee about the possible influence of hydrogen on both mechanical behavior and long-term aging.

This is the aim of the present paper. A tensile test machine was fitted with a pressurized hydrogen chamber to address (i) the possible coupling between hydrogen diffusion and tensile behavior and (ii) the influence of long-term exposure to hydrogen, on the mechanical response of semi-crystalline polymers. The work was based on two polymers already used for natural gas transport: a PE and a PA11. The pressure level (30 bars) was selected in accordance with gas networking standards. Microstructure changes were tracked by standard Differential Scanning Calorimetry (DSC).

2. Experimental

2.1. Materials

Two semi-crystalline polymers currently used for gas transport, a PE 100 and a PA11, have been tested in the as-received form (1 mm-thick extruded sheets) and after long-term aging in a pressurized hydrogen atmosphere (samples named "hydrogen-aged" in the following). As determined by DSC (following the protocol described below), PE exhibited a crystallinity ratio of 57% and a melting temperature of 130 °C. The alpha-c transition corresponding to the onset of mobility of conformational defects in the crystalline lamellae, usually located at $T\alpha_c = 60–80$ °C, could not be observed in DSC thermograms. In as-received PA11, the crystallinity ratio was 22%, the melting temperature was 189 °C and the glass transition temperature was 49 °C.

Before testing, as-received materials were conditioned at ambient humidity. Tensile tests were performed in dumbbell specimens machined in the extrusion direction with the geometry summarized in Table 1. "Hydrogen-aged" samples were machined with a hollow punch from 1-mm thick extruded sheets used in another part of the research program to perform hydrogen permeation experiments [31]. During these prior permeation experiments, PE and PA11 samples were maintained in a 100% H_2 atmosphere during various times (from 1 to 13 months) at three different temperatures (20, 50 and 80 °C) and two differential pressures between the sheet sides (5 and 2 MPa). Aging conditions are listed in Table 1. PA11 samples have been dried before the permeation experiments but maintained at ambient humidity between the end of permeation measurement and mechanical testing.

2.2. Differential scanning calorimetry

Standard DSC was used to characterize the microstructure. Samples (around 10 mg) were sealed in aluminum pans and continuously heated at 10 °C/min under nitrogen sweep. The percent crystallinity X_{DSC} was calculated from Equation (1):

$$X_{DSC} = 100 \times \frac{\Delta H_m}{\Delta H_m^0} \tag{1}$$

where ΔH_m is the energy required to melt the crystalline phase, determined from the endothermic melting peak area, and ΔH_m^0 the enthalpy of melting of the pure crystalline polymer (290 J/g for PE [32] and 226.4 J/g for PA11 [33]). The melting temperature was determined as the maximum of the melting peak.
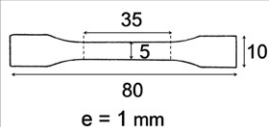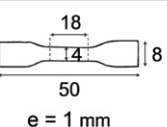
2.3. Mechanical tests under pressure

A tensile testing machine has been fitted with a pressurized-hydrogen chamber displaying pressures from the ambient up to 40 MPa. The gas chamber could be filled with nitrogen or hydrogen. All tests were carried out at 3 MPa, in accordance with gas distribution standard, and at "ambient" temperature, after equilibration of the sample to the surrounding air temperature before the test. However, due to safety standard linked to hydrogen explosibility, the testing machine was located in a well-aerated building and thus exposed to outdoor temperature variations from one day to another. Once stabilized, the temperature variation during the experiment was ±0.1 °C.

Still due to safety reasons, the volume of the hydrogen chamber was small (inner diameter 150 mm; deepness 100 mm) and moreover reduced by the grips volume. Then, short enough samples had to be tested to keep a sufficient displacement range: 23 mm for the shortest specimens (i.e. a maximal conventional strain of 125%) and 7 mm for the longest ones (i.e. a maximal conventional strain of 15%).

The axial force F, axial displacement of the cylinder d, temperature T and pressure P were monitored during the test. The axial force was recorded from a 20 kN load cell located between the cylinders. The load cell accuracy was 0.4% of the full range, i.e. ± 10N. Tensile tests were carried out at a constant displacement speed of the cylinder, i.e. at a constant conventional strain-rate. The Cauchy stress σ and the logarithmic strain ε were calculated from F,

Table 1
Geometry and aging history (temperature, pressure and duration) of samples.

as-received	aged into pressurized hydrogen atmosphere				
35 5 10 80 e = 1 mm	18 4 8 50 e = 1 mm		Temperature (°C)	Pressure (MPa)	Aging time (months)
		V1	80	2	9
		V2	20	2	13
		V3	80	0.5	13
		V4	80	2	1
		V5	50	2	13
		V6	20	0.5	13

d, the initial gauge length of the sample l_0 and the initial cross section area S_0, assuming a constant volume deformation.

The Young's modulus was calculated from a linear interpolation of the stress-strain curves between 0 and 1%/2% for PA11/PE respectively. The yield stress was defined as the maximal force point in softening curves and as the onset of the stress-hardening stage in consolidating curves.

Samples were tightened between grooved grips and maintained at nil force before testing. To avoid any dangerous mixture between hydrogen and oxygen from the ambient air after closure of the chamber, three successive pressurization/depressurization purging cycles were performed first, by introducing nitrogen up to 1 MPa. Simultaneous temperature raises and decreases (by a few degrees) were logically yielded. Then, the chamber was filled with hydrogen at a constant pressure rate of 0.6 MPa/min up to 3 MPa. The temperature raise was rather quick at the beginning and progressively equilibrated by the water circulating around the chamber and the load cell.

A constant pressure stage was imposed before testing, in order to equilibrate temperature (about 20 min long) and to complete hydrogen sorption.

The time needed to reach hydrogen saturation of the sample was estimated from a one-dimensional calculation through an infinite sheet of constant thickness e, i.e. by assuming that the other sample dimensions were much higher than the thickness and by neglecting diffusion through the lateral faces. Therefore, the calculated saturation time resulted overestimated. The hydrogen concentration at the top and bottom surfaces of the sheet $C_{\infty H2}$ was deduced from a Henry's law given by Equation (2):

$$C_{\infty H2} = P_{ext}S_g \tag{2}$$

where P_{ext} stands for the pressure of the surrounding gas and S_g represents the solubility, assumed to be temperature independent. Concentration is expressed as a volume ratio between the sorbed gas and the polymer (given in cm^3 (STP).cm^{-3} where STP stands for Standard conditions of Temperature (STP) (273K) and Pressure (0.1013 MPa). The initial hydrogen concentration within the sheet was assumed to be zero. The current global concentration $C(t)$ at any time t was obtained from the analytical solution in Equation (3), based on Fick's theory and proposed by Crank [34].

$$C(t) = C_{\infty H2}\left(1 - \frac{8}{\pi^2}\sum_{n=1}^{\infty}\frac{1}{(2n-1)^2}\exp\left(-(2n-1)^2\pi^2\frac{Dt}{e^2}\right)\right) \tag{3}$$

where D is the diffusion coefficient of hydrogen into PE or PA11 and e is the sheet thickness. Coefficients S_g and D were deduced from permeation tests performed in another part of the research program [35]. S_g values for PE at 40 °C and PA11 at 60 °C were respectively $3.6.10^{-7}$ and $4.29.10^{-6}$ cm^3 of gas (STP).cm^{-3} of polymer.Pa^{-1}. Values for D were $1.68\ 10^{-10}$ and $4.54\ 10^{-11}$ $m^2.s^{-1}$ for PE at 40 °C and PA11 at 60 °C respectively. 250 terms were retained for the calculation. Finally, the estimated time for hydrogen saturation of the entire specimen at 3 MPa was 1 h for both materials.

Upon loading/unloading of the sample, the temperature stabilized after about 40 min at a constant value (±0.1 °C). The ambient temperature in the chamber was not regulated and varied from one day to another between 16 and 29 °C. PA11, which glass transition temperature T_g is around 40 °C, was mostly bound to be sensitive to such fluctuations.

A constant cylinder displacement was imposed, corresponding to a constant conventional strain-rate of $8.6\ 10^{-3}\ s^{-1}$ for as-received samples and $1.6\ 10^{-2}\ s^{-1}$ for aged samples. The temperature kept stable all along the mechanical test (±0.1 °C). The chamber was depressurized at a constant pressure rate of 0.6 MPa/min, yielding a temperature decrease. For safety reasons again, the residual hydrogen was removed by three nitrogen purging cycles at 1 MPa before opening the chamber.

Similar tests have been carried out also in pressurized nitrogen and air at atmospheric pressure. The experimental protocol for nitrogen tests was very close to that applied for hydrogen, except for the final purging step which was needless. In this way, the mechanical history was the same for experiments under hydrogen and nitrogen. Sorption calculations with diffusion and solubility coefficients for nitrogen into PE [14] showed that the saturation regime was also reached after the 1-h step defined for the hydrogen protocol.

The reproducibility was estimated as a standard deviation from the mean value by repeating the same experiment between 3 and 6 times for each material and loading condition. The reproducibility of experiments in ambient air (including the experimental device precision, the dimensional variability of samples and material heterogeneity) was estimated from tests performed in as-received PE. The axial force scattering measurement over 6 tests was $\pm3.1\%$. A higher scattering was expected for PA11 due to the room temperature and moisture content variability; it was discussed in the following. The experimental error increased for pressure experiments due to sliding effects between cylinders and o-rings: the axial force
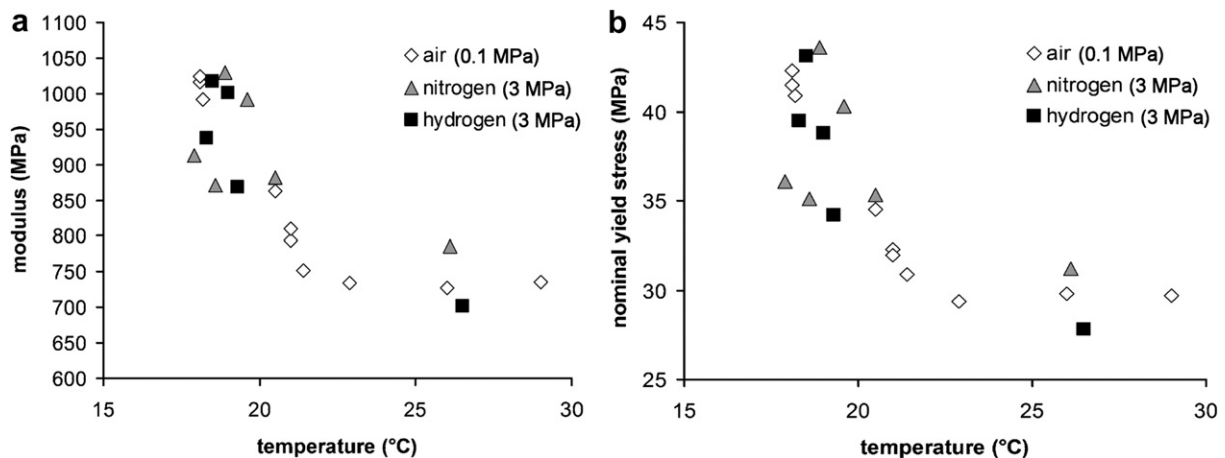

Fig. 1. Influence of the room temperature variability on the (a) Young's modulus and (b) yield stress in as-received PA11.
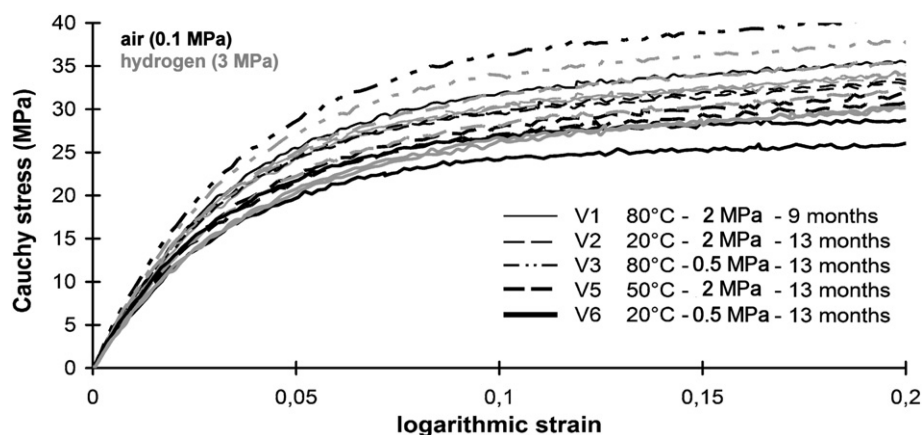
Fig. 2. Stress-strain curves obtained in PE in atmospheric air and 3 MPa hydrogen, after various aging histories (see Table 1).

scattering reached ± 10% for PE (4 tests). A more precise measurement of the mechanical load under hydrogen pressure would require larger specimens not really compatible with the small volume of the chamber.

3. Results and discussion

3.1. Coupling between hydrogen diffusion and tensile properties in as-received materials

A first series of tensile experiments were performed in as-received materials at ambient air, and under 3 MPa of hydrogen and nitrogen.

Concerning PE, differences between curves obtained in various environments could not be dissociated from the experimental scatter and no significant pressure effect could be evidenced. The Young's modulus was 954 ± 74 MPa (over 7 tests) in atmospheric air, 972 ± 57 MPa (over 4 tests) under 3 MPa of hydrogen and 978 ± 37 MPa (over 5 tests) under 3 MPa of nitrogen. The yield stress was respectively 27 ± 1 MPa, 26.6 ± 1.6 MPa and 27.8 ± 1.1 MPa. It means that, if existing, the hydrogen influence on the tensile behavior of PE at 18 °C did not exceed 10%.

Data obtained in PA11 with the same sample geometry were even more scattered. The same average analysis as conducted above in PE led to a Young's modulus of 845 ± 115 MPa (over 10 tests) in atmospheric air, 905 ± 130 MPa (over 5 tests) under 3 MPa of hydrogen and 915 ± 90 MPa (over 6 tests) under 3 MPa of nitrogen. The yield stress was respectively 34.3 ± 5 MPa, 36.7 ± 5.9 MPa and 37 ± 4.3 MPa. Like for any polymer close to the glass transition temperature T_g, the mechanical properties of PA11 were expected to vary with room temperature (i.e. around 30 °C below T_g). Moreover, polyamides are known to be hydrophilic and mechanically dependent on the water weight content. None of these two factors were regulated in the present study and the latter one could not even be accessed. However, the influence of temperature effect could be examined, as proposed in Fig. 1 by plotting the Young's modulus E and the yield stress σ_y against the ambient temperature measured for each test. Both E and σ_y expectedly dropped with the temperature raise and evolutions appeared reasonably correlated to the testing temperature. It clearly evidenced a major influence of the testing temperature on the tensile stress scattering, compared with any pressure or environment effect. In the same way as previously established for PE, coupling between hydrogen diffusion and tensile behavior appeared to be negligible.

3.2. Influence of long term aging in pressurized hydrogen

The goal was to evaluate the influence of aging parameters like temperature or hydrogen pressure on the tensile properties, coupled or not to hydrogen diffusion. To this aim, series of samples aged for several months in the conditions listed in Table 1 have been tested both in atmospheric air and pressurized hydrogen (3 MPa). Aging temperatures were 20 °C or 80 °C (meaning below and above T_g for PA11 respectively; and below and above $T\alpha_c$ for PE respectively), except for a few tests performed at an intermediate temperature of 50 °C.

Fig. 2 plots the tensile stress-strain curves recorded for aged PE samples. Let us focus first on the influence of hydrogen diffusion on the tensile behavior, by comparing tests performed in atmospheric air and 3 MPa hydrogen for each aging history. After annealing above $T\alpha_c$ (V1 and V3), ambient air curves were slightly above hydrogen curves, unlike after annealing below $T\alpha_c$ (V2, V5 and V6). However, differences were very fine, consistently with the scatter depicted above in as-received materials. DSC thermograms in PE samples after aging for 13 months at 20 °C (V2), 50 °C (V5) and 80 °C (V3) were compared in Fig. 3. The corresponding crystallinity ratio was 56.8, 57 and 60.5% respectively and the melting temperature equaled 130.2, 131.1 and 131 °C respectively. Unsurprisingly, annealing at increasing temperature led to better crystallized materials but consequences on the stress-strain behavior were minor than the experimental scatter. Any effect of the aging pressure could have aroused from the comparison of V2 (2 MPa) and V6
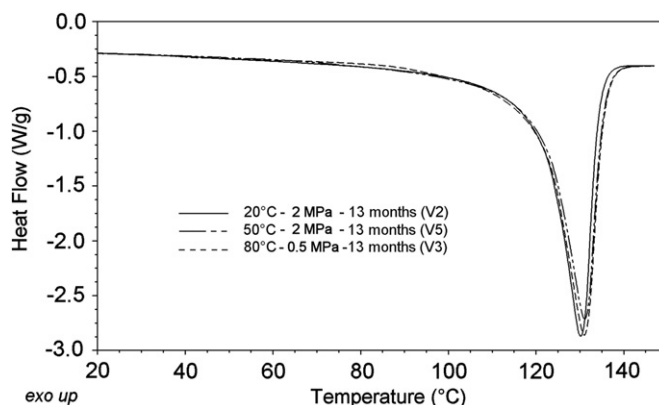

Fig. 3. DSC thermograms (first heating run; 10 °C/min) in PE samples aged for 13 months at 20 °C (V2), 50 °C (V5) and 80 °C (V3).
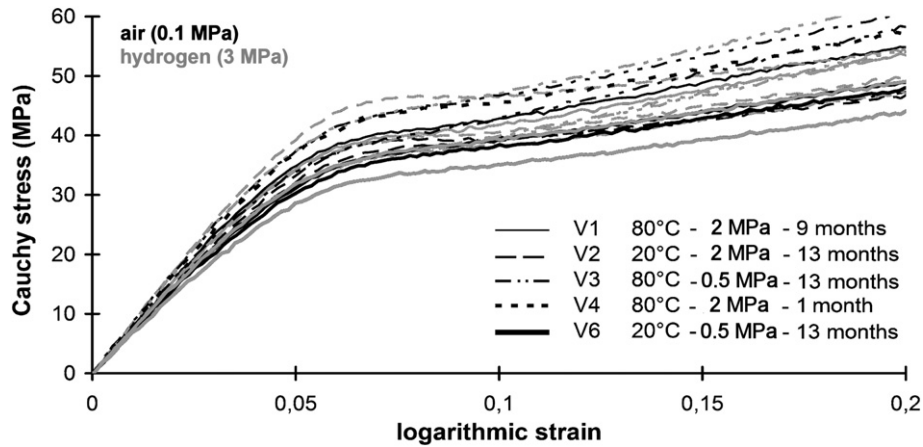
Fig. 4. Stress-strain curves in PA11 tested in atmospheric air and 3 MPa hydrogen after aging at various temperatures, durations, pressures and atmospheres.

(0.5 MPa) at 20 °C but the two series were too close together considering the tests reproducibility. Concerning the aging temperature influence, the stress level after aging at 0.5 MPa and 80 °C (V3) was rather clearly higher than after aging at 20 °C (V6). However, this difference was no more observed after aging at 2 MPa: all curves overlapped over a limited scatter range regardless the aging temperature of 20 °C (V2), 50 °C (V5) or 80 °C (V1). These results supported the weak influence of hydrogen diffusion coupling and aging processes.

The same series of tests in PA11 were presented in Fig. 4. Considering the wide scatter pointed out in as-received PA11, no evidence was brought from the comparison of tests performed in air or hydrogen after the same aging protocol. This emphasized the minor coupling effect previously pointed out in as-received materials. The aging time influence could be addressed by comparing 1-month (V4) and 9-months (V1) aging at 80 °C and 2 MPa of hydrogen: the scatter between the two curves was not significant again. The influence of hydrogen pressure during aging was also negligible, as deduced from the comparison between 2 MPa (V2) and 0.5 MPa (V6) experiments at 20 °C. The V2 curves were slightly above the V6 ones but the difference results less noticeable than previously observed for PE. Let us consider finally the aging temperature effect. Unlike in PE, only two series of curves (V3 and V6) could be compared to keep constant the aging pressure and time. Under the same aging

pressure (0.5 MPa) and after 13 months, aging at 80 °C resulted in a stiffer behavior than aging at 20 °C. Such a result was pointed out for PE. In the same way as for PE under 2 MPa, and despite variable aging times, all V2 (20 °C; 13 months) and V1 (80 °C; 9 months) curves laid within the experimental scatter.

In many ways, trends did not appear very convincing regarding the large scatter previously pointed out in as-received specimens. Furthermore, correlation to the ambient temperature was worth being examined here again, as displayed in Fig. 5. Both E and σ_y monotonically decreased for increasing room temperature regardless aging conditions. Here again, the principal influence dealt with ambient temperature variability. Fig. 6a showed the corresponding first heating run of DSC experiments carried out after one month at 80 °C in air (atmospheric pressure), vacuum and hydrogen (3 MPa). Aging in vacuum aimed at separating the oxidation effect bound to affect PA11 when annealed in air at high temperature. Firstly, the glass transition could not be detected very precisely, due to the overlapping endothermic peak yielded by the physical aging occurring between the end of the aging protocol and the DSC experiment. It seated at about 45 °C for all samples. Secondly, another endothermic peak could be distinguished at around 90–95 °C: it is linked to the annealing at 80 °C [8]. Finally, the melting peak of primary crystals was not significantly modified. The melting temperature after aging in vacuum (190.4 °C) was
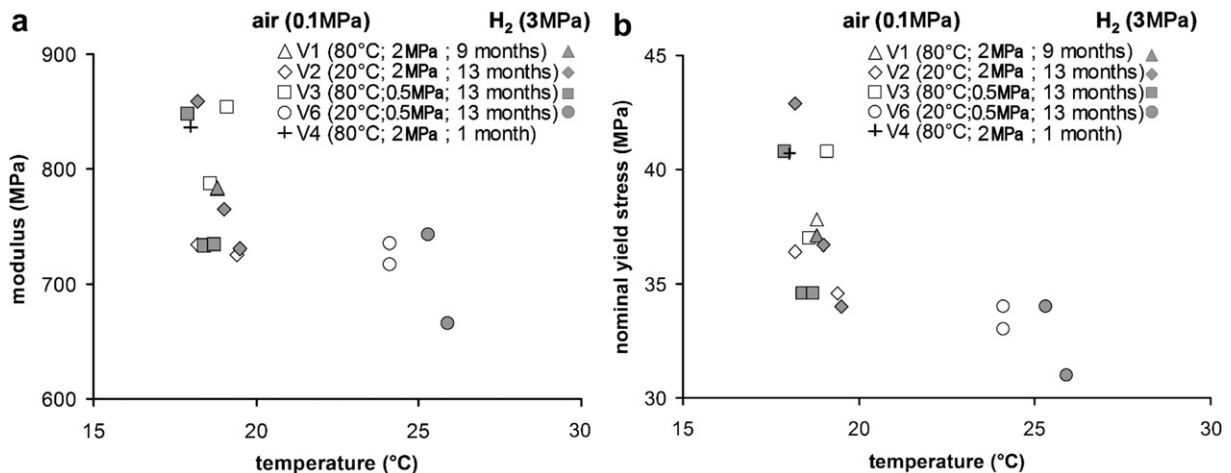

Fig. 5. Relationship between (a) Young's modulus, (b) yield stress and room temperature in PA11 samples after various aging protocols in hydrogen (temperature, pressure, duration).
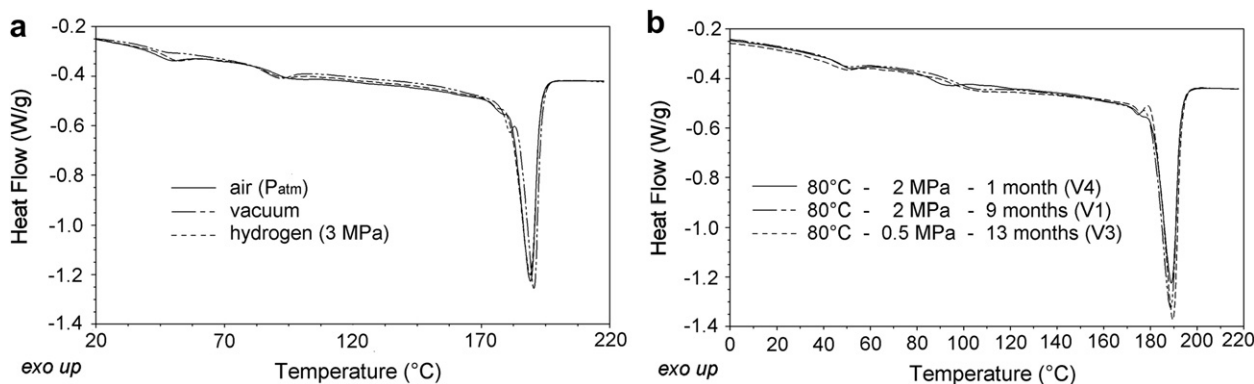
Fig. 6. DSC thermograms in PA11 (a) After aging for one month at 80 °C in several atmospheres and (b) After variable aging times in hydrogen at 80 °C.
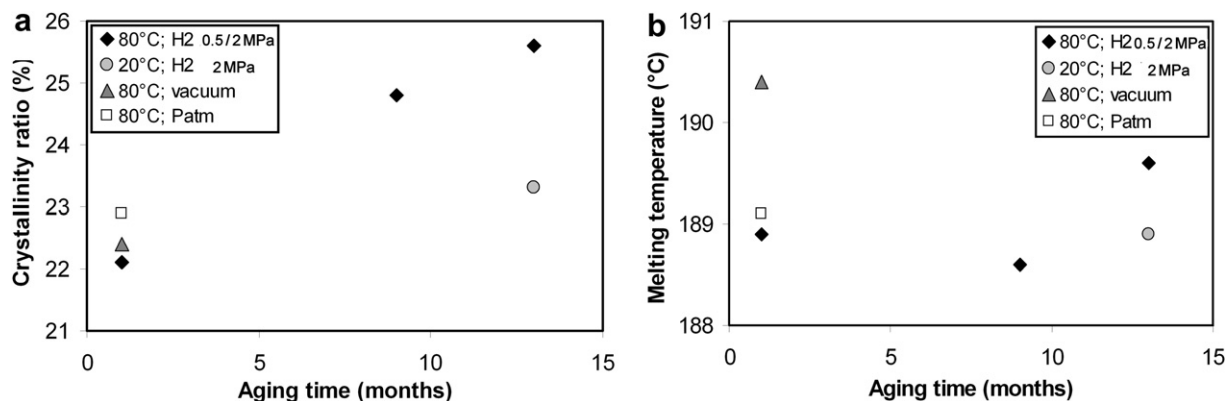

Fig. 7. Time dependence of the crystallinity ratio and melting temperature measured from DSC thermograms in PA11 (first heating run; 10 °C/min) after variable aging history.

slightly higher than in air (189.1 °C) or hydrogen (188.9) but the crystallinity ratio was nearly identical (22.9%, 22.4% and 22.1% in air, vacuum and hydrogen respectively).

Fig. 6b displayed thermograms obtained in samples annealed in hydrogen for 1 month (V4), 9 months (V1) and 13 months (V3). The aging pressure was 2 MPa, except for the latter test (0.5 MPa). The glass transition was unaffected by the time spent in pressurized hydrogen prior to the DSC experiment. The endothermic peak observed slightly above the annealing temperature (80 °C) was shifted towards higher temperatures with the annealing time. This was consistent with previous results in the same material [2]: a longer annealing yielded a better local re-organization of the constrained amorphous phase which further needed more energy −and therefore a higher temperature− to be destroyed.

Characteristics of the melting peak of primary crystals, i.e. the crystallinity ratio and the melting temperature, were plotted in Fig. 7 for various aging protocols. The melting peak was always centered on roughly the same melting temperature but its deepness increased with aging time. The associated crystallinity ratio logically increased. However, by comparing tests after aging for 13 months at 20 and 80 °C, the phenomenon seemed to be related more to temperature than to hydrogen atmosphere.

4. Conclusions

Coupling between gas diffusion and mechanics in polymers is bound to modify their mechanical properties and some aging processes due to long time gas exposure could be activated. In-situ experiments were needed to address such effects. However, concerning hydrogen atmosphere, very few experimental works have

been reported. The purpose of this study was to provide new experimental data for the design of polymer parts sustaining hydrogen atmosphere, based on mechanical tensile experiments in pressurized hydrogen or nitrogen atmosphere. Two semi-crystalline polymers (PE and PA11), currently used for gas distribution networking, have been studied. A noticeable experimental scatter aroused from the small force level compared to the load cell capacity and from frictional forces due to the pressurization device. However, tests performed in PE in atmospheric air and hydrogen at 3 MPa showed a negligible coupling between mechanics and hydrogen diffusion. The same result held for PA11 materials, for which the ambient temperature scatter appeared of first importance compared to a possible hydrogen effect.

After long-term aging up to 13 months in hydrogen at various pressures (5 or 2 MPa) and temperatures below and above the glass transition of PA11 and the alpha-c transition for PE (20 °C, 50 °C and 80 °C), no deleterious effect was observed on the mechanical properties of PE and PA11. Differences observed for PA11 essentially resulted from testing temperature variability close to the glass transition temperature.

Consistently with the tensile properties, no significant evolution of the crystalline microstructure after aging in hydrogen aroused from DSC experiments. Again, the clearer effect was associated with the annealing temperature in PA11.

References

[1] Koutský J, Šplíchal K. Hydrogen and radiation embrittlement of CrMoV and CrNiMoV ferritic RPV steels. Int J Press Vessels Pip 1986;24(1):13–26.

[2] Yokogawa K, Fukuyama S, Kudo K, Shewmon PG. Effect of hydrogen attack on tensile and creep properties of low carbon steel. Int J Press Vessels Pip 1989; 37(5):365–85.

[3] Murakami Y. The effect of hydrogen on fatigue properties of metals used for fuel cell system. Int J Fract 2006;138:167–95.

[4] Krom AHM, Bakker A, Koers RWJ. Modelling hydrogen-induced cracking in steel using a coupled diffusion stress finite element analysis. Int J Press Vessels Pip 1997;72(2):139–47.

[5] Taha A, Sofronis P. A micromechanics approach to the study of hydrogen transport and embrittlement. Eng Fract Mech 2001;68:803–37.

[6] Kotake H, Matsumoto R, Taketomi S, Miyazaki N. Transient hydrogen diffusion analyses coupled with crack-tip plasticity under cyclic loading. Int J Press Vessels Pip 2008;85(8):540–9.

[7] Alshisaka A, Kawagoe M. Examination of the time-water content superposition on the dynamic viscoelasticity of moistened polyamide 6 and epoxy. J Appl Polym Sci 2004;93:560–7.

[8] Weibina Gao, Shimina Han, Minjiaoa Yang, longa Jang, Yi Dan. The effects of hydrothermal aging on properties and structure of bisphenol A polycarbonate. Polym Degrad Stab 2009;94(1):13–7.

[9] Bellinger MA, MacKnight WJ. Effects of water on the mechanical relaxation in polyamide-4. Acta Polymerica 1995;46(5):361–6.

[10] Perry JD, Nagai K, Koros WJ. Polymer membranes for hydrogen separations. MRS Bull 2006;31:745–9.

[11] Stodilka DO, Kherani NP, Shmayda WT, Thorpe SJ. A tritium tracer technique for the measurement of hydrogen permeation in polymeric materials. Int J Hydrogen Energy 2000;25:1129–36.

[12] Shishatskiy S, Nistor C, Popa M, Nunes SP, Peinemann KV. Polyimide asymmetric membranes for hydrogen separation: influence of formation conditions on gas transport properties. Adv Eng Mat 2006;8:390–7.

[13] Compan V, Lopez-Lidon M, Andrio A, Riande E. Macromol 1998;31:6984–90.

[14] Flaconnèche B, Martin J, Klopffer MH. Permeability, diffusion and solubility of gases in polyethylene, polyamide 11 and Poly(vinylidene fluoride). Oil Gas Sci Technol – Rev IFP 2001;56:261–78.

[15] Struik LCE. The mechanical and physical aging of semicrystalline polymers. Polymer 1987;28(9):1521–33.

[16] Castagnet S, Thilly L. High-pressure dependence of structural evolution in polyamide 11 during annealing. J Polym Sci 2009;47:2015–25.

[17] Hu CC, Fu YJ, Hsiao SW, Lee KR, Lai JY. Effect of physical aging on the gas transport properties of poly(methyl methacrylate) membranes. J Membr Sci 2007;303:29–36.

[18] Lin WH, Chung TS. Gas permeability, diffusivity, solubility, and aging characteristics of 6FDA-durene polyimide membranes. J Membr Sci 2001;186: 183–93.

[19] Basfar AA, Idriss Ali KM. Natural weathering test for films of various formulations of low density polyethylene (LDPE) and linear low density polyethylene (LLDPE). Polym Degrad Stab 2006;91(3):437–43.

[20] Radhakrishnana CK, Alexb R, Unnikrishnanc G. Thermal, ozone and gamma ageing of styrene butadiene rubber and poly(ethylene-co-vinyl acetate) blends. Polym Degrad Stab 2006;91(4):902–10.

[21] McCourt MP, McNally GM, Murphy WR, McNally T. Proceedings 58th Annual Technical Conference of the Society-of-Plastics-Engineers ANTEC 2000, Orlando. A study of the deterioration in the mechanical performance of polymers used in multilayer fuel lines with immersion in a standard automotive test fuel, vol. I–III; 2000. pp. 2646–2651.

[22] Merdas I, Thominette F, Verdu J. Hydrolytic ageing of polyamide 11—effect of carbon dioxide on polyamide 11 hydrolysis. Polym Degrad Stab 2003;79(3): 419–25.

[23] Wheltona AJ, Dietrich AM. Critical considerations for the accelerated ageing of high-density polyethylene potable water materials. Polym Degrad Stab 2009; 94(7):1163–75.

[24] Weon JI. Effects of thermal ageing on mechanical and thermal behaviors of linear low density polyethylene pipe. Polym Degrad Stab 2010;95(1): 14–20.

[25] Escudero Acevedoa M, Quijadaa R, Campos Vallette M. Thermal oxidation of metallocene ethylene-1-olefin copolymer films during one year oven aging. Polym Degrad Stab 2008;93(10):1947–51.

[26] Mueller W, Jakob I. Oxidative resistance of high-density polyethylene geomembranes. Polym Degrad Stab 2003;79(1):161–72.

[27] Alchikh M, Fond C, Frere Y. Discontinuous crack growth in poly (vinyl fluoride) by mechanochemical ageing in sodium hydroxide. Polym Degrad Stab 2010;95(4):440–4.

[28] Qian R, Lu X, Brown N. The effect of concentration of an environmental stress cracking agent on slow crack growth in polyethylenes. Polymer 1993;34(22): 4727–31.

[29] Roy A, Gontcharova-Benard E, Gacougnolle JL. Hygrothermal effects on failure mechanisms of composite/steel bonded joints. Proceedings Symposium on time dependent and Nonlinear effects inPolymers and composites, Atlanta 1998. ASME Tech Public 2000;135:353–71.

[30] Olivier L, Baudet C, Bertheau D, Grandidier JC, Lafarie-Frenot MC. Development of experimental, theoretical and numerical tools for studying thermo-oxidation of CFRP composites. Composites Part A 2009;40(8): 1008–16.

[31] Pocachard J. Internal report. ANR Program PAN'H-PolHYTube; 2009.

[32] Wünderlich B. Macromolecular Physics. In: Crystal structure, Morphology, defects, vol. 1. New-York: New York Academic Press; 1973.

[33] Inoue M. Studies on crystallization of high polymers by differential thermal analysis. J Polym Sci 1963;1:2697–709.

[34] Crank J. The mathematics of diffusion. Oxford: Clarendon Press; 1956.

[35] Klopffer MH. Internal report. ANR Program PAN'H-PolHYTube; 2009.